Electrochemical Point-of Care (PoC) Determination of Interleukin-6 (IL-6) Using a Pyrrole (Py) Molecularly Imprinted Polymer (MIP) on a Carbon-Screen Printed Electrode (C-SPE)

M. de Lurdes Gonc¸alves[a,c], Liliana A. N. Truta[a,c], M. Goreti F. Sales[b,c], and Felismina T. C. Moreira[a,c]

[a] BioMark/ISEP, School of Engineering, Polytechnic of Porto, Porto, Portugal; [b] BioMark/UC, Faculty of Sciences and Technology, University of Coimbra, Coimbra, Portugal; [c] CEB, Centre of Biological Engineering, Minho University, Braga, Portugal

ABSTRACT

Here is presented a highly sensitive biomimetic sensor for the detection of an Alzheimer's Disease (AD) biomarker, interleukin-6 (IL6), for point-of-care (PoC) analysis. The imprinted polymeric film was prepared by the co-electropolymerization of pyrrole (Py) and carboxylated pyrrole in the presence of IL6, on a carbon-screen printed electrode . The biomarker molecule was then removed by oxalic acid , creating the recognition vacant sites. Similarly, a control was also prepared in absense of the IL6 biomarker . The different steps of the sensor fabrication were characterized by Raman Spectroscopy, Electrochemical Impedance Spectroscopy (EIS), and Cyclic Voltammetry. Biomarker recognition and capture capacity of the sensing material was measured by EIS. The biomimetic sensor showed a limit of detection for IL6 of 0.02 pg/mL in spiked serum samples. Overall, the biosensing device showed good sensitivity, reproducibility, accuracy, and rapid response time, which contibute for the development of early diagnostics Poc tools for neurological diseases.

KEYWORDS

Carbon-screen printed electrode (C-SPE); cyclic voltammetry (CV); electrochemical impedance spectroscopy (EIS); Interleukin-6 (IL-6); point-of care (PoC) biosensor; pyrrole (Py) molecularly imprinted polymer (MIP)

Introduction

Inflammatory processes are associated with an extensive range of disorders and conditions which, strongly influence the levels of certain biomolecules in the human body . These mecahnisms and/or responses can be characterized as acute (short-lived) or chronic (permanent responses) typically associated to autoimmune diseases. Cytokines are an example of biomolecules that tend to increase with inflammatory responses. Several cytokines have been identified as inflammation biomarkers, such as tumor necrosis factor alpha (TNF-a) (involves macrophages, T cells, and NK cells), interleukin-1 beta (IL-1b) (macrophages and epithelial cells) and interleukin-6 (IL6) (macrophages, T cells, and endothelial cells) (Cross et al. 2017; Day et al. 2018; Janelidze et al. 2018; Suk 2006). Additionally, the growing scientific evidences confirmed the relevance

between inflammation and dementia, being the most common and irreversible condition, Alzheimer's disease (AD). Recent studies have shown that Alzheimer's patients with cytokine overexpression experienced an increase of both oxidative and nitrosative stress, as well as autoimmune responses (Balducci et al. 2018; Cabinio et al. 2018; Finneran and Nash 2019; Janelidze et al. 2018; Marttinen et al. 2018; Popp et al. 2017). In dementia, pathophysiological changes, in a neurological context, may be develop decades before the appearance of the first symptoms. Thus, an early diagnosis of such diseases may prevent or minimize neurodegenerative alterations. Although few validated dementia biomarkers were already identified, several dementias are still lacking biomarkers. This added to the difficulty in monitoring biomarkers in peripheral fluids makes early diagnosis a great challenge. Some cytokines such as TNF-a or IL6 are regulated by neuro-inflammatory processes associated with neurodegenerative disorders (Berkenbosch et al. 1992). The levels of these cytokines may be an indicator of neuroinflammation in Alzheimer's disease Currently, ELISA and Western blotting are the gold standard methods for IL-6 detection. However, these techniques are time consuming, requiring sophisticated instrumentation.

Biosensing devices offer advantages compared with the traditional methodologies in terms of design simplicity and low cost. Other advantages are their robustness, easy miniaturization, and suitability for small volume analysis. Several biosensing devices have been reported for the point-of-care (PoC) detection of IL6 based on electrochemical (Huang et al. 2015; Huang et al. 2013; Liu et al. 2013; Lou et al. 2014; Ojeda et al. 2014; Tsuneyasu et al. 2014), electroluminescence (Liu et al. 2013) and optical transduction methods (Tsuneyasu et al. 2014; Wang et al. 2010) demonstrating good analytical performance in terms of the limit of detection (LOD). Most of these methods use natural compounds as biorecognition element, such as antibodies or enzymes, which have clear disadvantages in terms of price and reduced stability under harsh pH and temperature conditions.

Alternatively, several electrochemical biosensors have employed aptamers as biorecognition element (Chen et al. 2020; Khosravi, Loeian, and Panchapakesan 2017; Terti¸s et al. 2017; Terti¸s et al. 2019) for IL6 detection . Aptamers are oligonucleotide sequences that recognize the analyte with good sensitivity and selectivity. However, the main difficulty of aptamer based diagnostics is related to the absence of standardized protocols for their synthesis (Lakhin, Tarantul, and Gening 2013).

Molecular imprinting technology is able to overcome these limitations due its promising properties of robustness at harsh pH and temperature, reusability, price, and stability (Algieri

et al. 2014; Chen et al. 2016; Frasco et al. 2017; Haupt et al. 2012; Ribeiro et al. 2018; Uzun and Turner 2016). Different strategies for the synthesis of molecular imprinting polymers have been reported in the literature for proteins, including radical polymerization (Cabral-Miranda, Gidlund, and Sales 2014; Moreira et al. 2013), atom transfer radical polymerization (Li et al. 2014), photo-polymerization (Chen et al. 2015), and electropolymerization (ELP) (Frasco et al. 2017; Gomes et al. 2018; Ribeiro et al. 2018; Tavares and Sales 2018). ELP shows special benefits, regarding thickness control of the film and porosity which, can be tunned by changing the electrochemical parameters. In addition, this approach is simple, rapid, and inexpensive to perform.

Here, we described an ultrasensitive molecular imprinted polymer developed on a carbon screen printed electrode (C-SPE) for PoC detection of IL6. The polymer is formed by electrosynthesis of the pyrrole (Py) and carboxylated pyrrole (Py-COOH) at near physiological conditions with the biomarker trapped in the polymeric matrix. Upon target removal with acidic treatment, the imprinted sites are the available to recapture the imprinted molecule. In parallel, a control material (NPPy) was prepared without recognition imprinted binding sites. To our best knowledge, this work describes for the first time the synthesis of a molecular imprinting polymer for electrochemical detection of IL6 at the fg/mL level in serum samples. Overall, this biosensing material has shown promising results for PoC neuro-inflammatory biomarker detection. Moreover, the presence of biomarkers capable of predicting cognitive decline are of great value for the development of preventive therapies.

Experimental

Apparatus

The electrochemical measurements were conducted using a PGSTAT302N potentiostat/galvanostat from Metrohm Autolab. Carbon screen-printed electrodes (C-SPEs) were purchased from Dropsens (DRP-C220AT), with working and counter electrodes made of carbon and reference electrode and electrical contacts made of silver. The diameter of the working electrode was 4 mm and the C-SPEs were placed in a suitable switch box, interfacing the electrical contacts of the C-SPE with the electrical connections of the potentiostat/galvanostat.

Raman spectra were collected using a Thermo Scientific DXR Raman microscope equipped with a 532 nm laser. A 5 mW laser power on the sample was used with a 50 lm slit aperture.

Reagents

All chemicals were of analytical grade and water was deionized or ultrapure Milli-Q laboratory grade. Pyrrole; sodium chloride (KCl); pyrrole-2-carboxylic acid, 99%; and oxalic acid dihydrate (OxAc) were purchased from Merck. Phosphate buffered saline (PBS); potassium hexacyanoferrate III ($K_3[Fe(CN)_6]$); and IL6 (Human, recombinant animal component free) were obtained from Fluka; and potassium hexacyanoferrate II trihydrate ($K_4[Fe(CN)_6]\cdot 3H_2O$) from Riedel-de-H€aen.

Electrochemical procedures

Electrochemical assays were performed in triplicate and evaluated in 5.0mM $[Fe(CN)_6]^{3/4}$ in 0.1M KCl. Cyclic voltammetry (CV) was performed using a potential range from 0.4 to 0.7V at a scan-rate of 50mV/s. Electrochemical impedance spectroscopy (EIS) was performed with $[Fe(CN)_6]^{3-/4-}$ solution in open circuit potential (OCP), using a sinusoidal potential perturbation with an amplitude of 0.1V across a frequency range from 0.1 to 100kHz. The impedance results were fitted with the NOVA commercial software.

Calibration curves were performed by EIS measurements for IL6 increasing concentrations ranging from 0.02 pg/mL to 2.0 mg/mL. Each concentration of IL6 standard solution was prepared in pH 6.0 PBS buffer and incubated on the imprinted sensor (MPPy) surface for 30 min, at room temperature. Serum analysis was done by spiking IL6 100-fold diluted in PBS buffer.

Plastic antibodies on the C-SPE

The molecularly-imprinted material was electropolymerized on the C-SPE after electrode pretreatment. The C-SPEs were prepared by chronoamperometry in 0.1 M KCl, for 200 s, at 1.7 V (Figure 1A).

The imprinting assay included two steps. The first step created the imprinted sites by protein interactions with a charged monomer (Py-COOH) by hydrogen bonds. A mixture of 10 mL of the IL-6 analyte (2 mg/mL), 45 mL Py (0.01 M) and 45 mL Py-COOH (20 mg/mL) were mixed and allowed to interact for 30 minutes to establish the hydrogen bonds between the protein and the Py-COOH. Next, 70 mL of the mixture were dropcasted on the electrode surface and incubated for 5 minutes. The CV polymerization (Figure 1B) was performed from 0.8 to 0.8 V at a scan-rate of 50 mV/s for 10 cycles. The NPPy material was prepared, in parallel, with the same procedure in the absence of the template. The Py concentration, potential range, scan-rate, and number of cycles were optimized. The optimum conditions of ELP were selected based on the stability of surface of the sensor and the electron transfer resistance (Figure S1).

The resulting biomimetic material was carefully rinsed with deionized water and incubated for 3 h in 0.05 M oxalic acid dihydrate to remove the target protein from the PPy. Next, to equilibrate the pH, the sensor was incubated for 30 min in PBS buffer at pH 7.4. In order to remove the residual monomers, the sensor was treated by CV, from 0.3 V to 0.3 V, for 10 cycles, at a scan-rate of 50 mV/s, in pH 6.0 PBS buffer.

Results and discussion

Optimization of the polymerization

In molecular imprinting, the thickness and the stability of the polymer are important parameters to reach accurate and sensitive sensing. The binding cavities and the stability of the polymer are affected by the monomer concentration, potential window of polymerization, number of cycles, and scan-rate (Sayyah, Abd El-Rehim, and El-Deeb 2003). In this work, the optimum electrochemical conditions were based on the surface stability and charge transfer resistance data. Overall, the best analytical performance in terms of stability of the polymeric material was achieved with 10 cycles of electropolymerization, at 50 mV/s, a 0.01 M monomer concentration, and a potential window from 0.8 to 0.8 V (Figure S1).

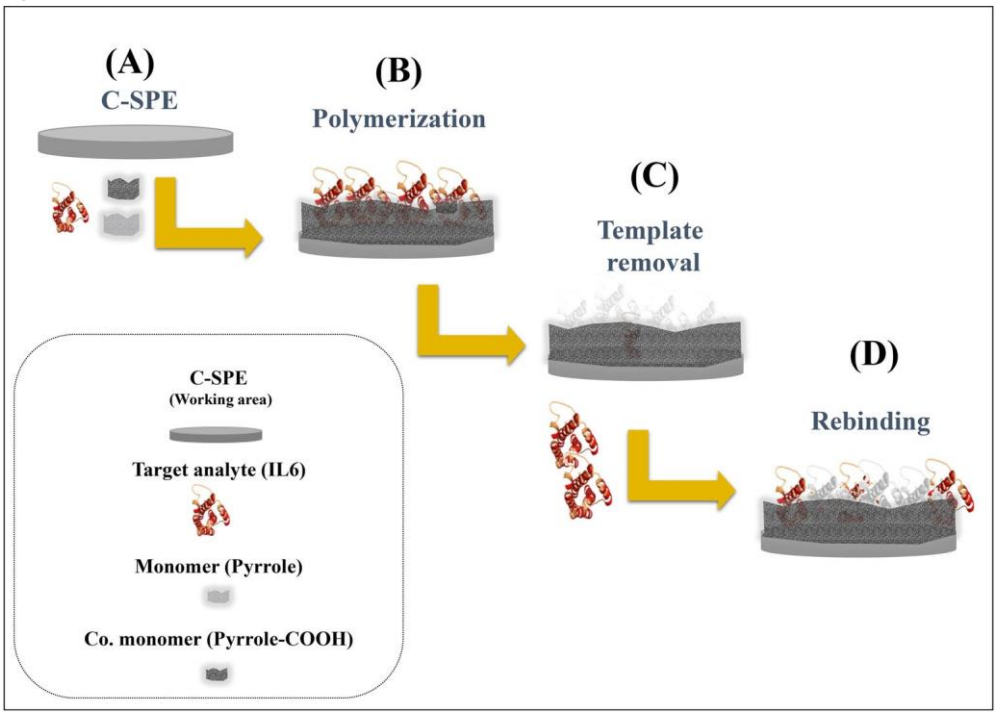

Figure 1. Preparation of the biomimetic biosensor using a carbon-screen printed electrode (C-SPE).

Molecular imprinting polymer fabrication

The synthesis of the molecularly-imprinted material involved the self-assembly of the charged monomer, Py-COOH, around the IL6 template; imprinting stage by the Py and Py-COOH electropolymerization; and template removal by oxalic acid (Figure 2).

The imprinting process started with the self-organization of a charged monomer, PyCOOH, around the IL6 molecule. This step promoted electrostatic interactions between IL6 and monomer. Next, the monomers were electropolymerized on the C-SPE surface, at pH 6.0, by consecutive CV scanning, using the conditions selected in the previous section. Lastly, the protein was separated from the PPy film by oxalic acid treatment. The electron transfer properties of the surfaces were characterized by EIS and CV, as shown in Figure 2.

The cyclic voltammograms of the iron redox probe for C-SPE with MPPy and NPPy polymeric films on the working electrode confirmed the presence of an insulating film (Figure 2). After electropolymerization, the redox peaks for the clean electrode almost disappeared compared to the redox probe measurements due to an irreversible electrochemical process from the blocked surface.

The electrical variations at the SPEs, due to electropolymerization, were also characterized by EIS. Overall, the electrochemistry data at the electrode-solution interface correlated well with the simplified Randle's cell (Daniels and Pourmand 2007) composed by a resistor (solution resistance, R_s) in series with a parallel circuit, a resistor (charge transfer resistance, R_{ct}) and a double layer capacitance (C_{dl}). The pretreated C-SPE presented very low charge transfer resistance compared to the polymer on the electrode

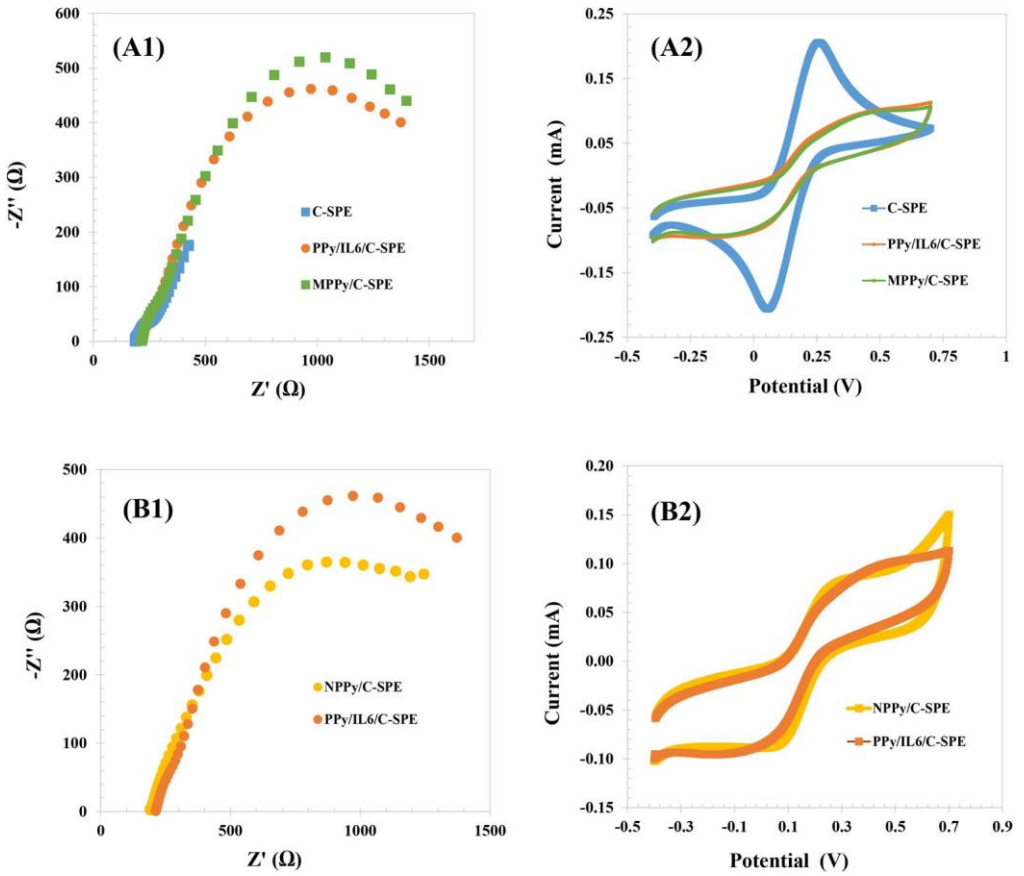

Figure 2. EIS (left) and CV (right) measurements for the synthesis of the biomimetic based sensor in 5.0 mM $[Fe(CN)_6]^{4/3}$ and 0.1 M KCl. Definitions: C-SPE, carbon-screen printed electrode; PPy, polypyrrole; IL6, interleukin 6; MPPy, imprinted sensor; and NPPy, non-imprinted material.

surface. The polymer on the carbon surface considerably increased the charge-transfer resistance of the C-SPE, resulting from the insulating features of the produced material, under the employed pH and electropolymerization conditions.

In addition, the NPPy control material was prepared in the absence of the protein IL6 during electropolymerization. The control provided a lower charge transfer resistance, when compared to the MPPy, due to the presence of IL6 in the polymer. The presence of IL6 in the polymer was expected to affect the electrical properties of the electrode, due to its intrin.

The target protein was removed from the polymeric matrix by oxalic acid treatment. This chemical treatment, modified the electrical features of the redox probe due the absence of the protein in the polymer. After acidic treatment, an increase in the charge transfer resistance was observed in MPPy. Usually, protein removal from the polymer tend to decrease the resistance. However, this phenomenon is also associated with protein protonation compared to the redox probe structure of the polymer and polymer

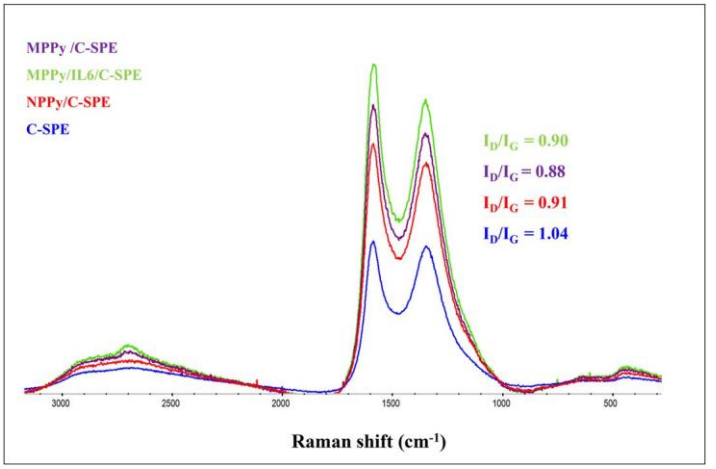

Figure 3. Raman spectra of the C-SPE, MPPy and NPPy materials. Definitions: C-SPE, carbon-screen printed electrode; MPPy, imprinted sensor; and NPPy, non-imprinted material.

structure modification due the presence of the cavities. If IL6 is positively protonated, the concentration of the iron redox probe at the surface may increase due to ionic interaction, thereby decreasing the charge transfer resistance. Additionally, PPy polymers retain alternating single (r) and double (p) bonds. Following template removal, the p-conjugated systems are broken as the entrapped protein leaves the polymer, hindering electron transfer through the polymer. Hence, decrease in the charge transfer resistance was observed for the MPPy calibrated in pH 6.0 PBS buffer.

Characterization by Raman spectroscopy

The structures of C-SPE, MPPy, NPPy, and MPPy after template removal were investigated by Raman spectroscopy, as shown in Figure 3.

Typical carbon peaks are shown in the Raman Spectra at 1351.3 cm^1 and 1590.4 cm^1 due to the disorder mode (D-band) and tangential mode (G-band), respectively. The ratio of D/G (I_D/I_G) band intensity corresponds to the atomic ratio between sp^3 and sp^2 carbons by the evaluation of graphite degree of disorder (Figure 4).

The calculated I_D/I_G ratio of C-SPE was 1.04. After polymerization of the NPPy and MPPy, the I_D/I_G ratio was reduced to 0.91 and 0.90, respectively. Overall, a decrease in the defect band D observed after polymerization is an indicator that the modification of C-SPE provides a more organized carbon material. As expected, the polymeric-based sensors (MPPy and NPPy) provided similar I_D/I_G ratios, which was expected based on the chemical similarity of these films.

After the removal of IL6 from the PPy film by chemical treatment with oxalic acid, a further decrease in the defects is observed, as I_D/I_G is 0.88. This phenomenon is due to the absence of the protein, that may introduce defects in the hexagonal structure of carbons in the polymer (Figure 3).

Overall, the Raman spectra confirm the structural changes between the control and the polymeric materials, thereby confirming the PPy layer on the carbon electrode.

Analytical performance of the sensor

The analytical performance of the biomimetic sensor was evaluated by calibration curves. The sensors were incubated for 30 minutes in each standard solution of IL6 protein and evaluated by EIS. Calibration curves obtained for the MPPy and NPPy sensors were plotted as the charge transfer resistance versus the logarithm of IL6 concentration from 0.02 pg/mL to 20 ng/mL. The charge transfer resistance of the MPPy decreased linearly with increasing IL6 concentration higher than 0.1 pg/mL (Figure 4). The average slope was 0.0601 kXmL/log[IL6, ng/mL] with a correlation coefficient exceeding 0.985 and a limit of detection lower than 0.1 pg/mL. The decrease in signal after IL6 protein incubation may be associated with the net charge of the protein. The isoelectric point (PI) of IL6 is approximately 6.96 (Khosravi, Loeian, and Panchapakesan 2017) and the pH of the buffer was 6.0. Hence, the number of positive and negative charges in the outer protein surface are equivalent due the proximity of the isoelectric point and pH. The positive charges of the protein on the surface, are likely to attract the redox probe to the electrode surface, as the redox probe is negative. A decrease in the charge transfer resistance was observed after protein incubation in Figure 4. The NPPy displayed random responses for the same protein concentrations, confirming that protein binding at the MPPy sensor is associated with the recognition cavities in the polymer. The relative standard deviation of repeated measurements was bellow 5%.

Analytical performance of the sensor with spiked serum

IL6 in plasma and cerebrospinal fluid has been identified as a potential biomarker, although its screening in plasma, results in a less invasive sample (Park, Han, and Mook-Jung 2020; Wu et al. 2015). Because of this promising possibility, lyophilized human serum was selected to characterize the applicability of the sensor and the selectivity for real sample analysis. In order to investigate the analytical response of the IL6 in spiked serum samples, the sensing material was incubated for 30 minutes at various

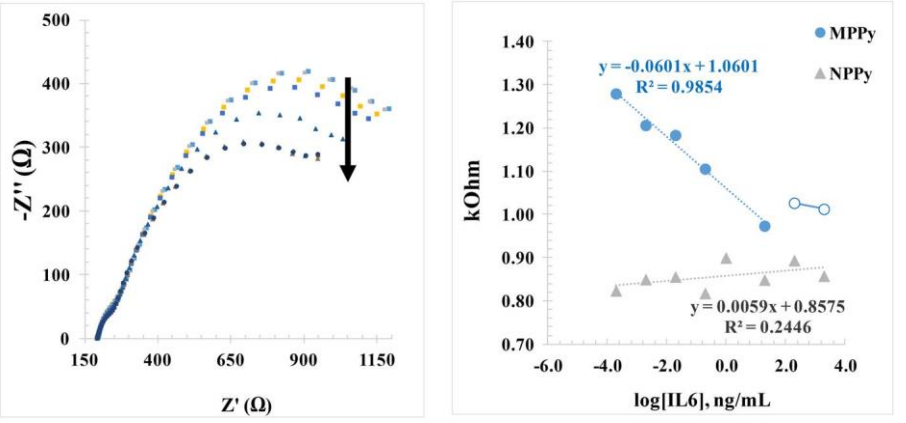

Figure 4. (A) EIS measurements of the MPPy based biosensor. (B) Calibration curves obtained for the non-imprinted polymer (NPPy, orange dots) and imprinted polymer (MPPy, blue dots) biosensor in PBS buffer at pH 6.0 in 5.0 mM $[Fe(CN)_6]^{4/3}$ and 0.1 M KCl, at IL6 concentrations of 0.02, 0.2, 2.0, 20, 200,2000, 20000 pg/mL.

Table 1. Comparison of the developed biosensor with electrochemical devices reported in the literature.

Electrochemical Technique	Recognition element	Linear Range	Sample application	Reference
Amperometry	Antibody	20-4000 pg/mL	Serum	Munge et al. 2009
Amperometry	Antibody	4-800 pg/mL	Serum	Wang et al. 2011
ASV	Antibody	0.1-100 pg/mL	Serum	Zhang et al. 2011
SWV	Antibody	0.01-0.1 pg/mL	Serum	Shi et al. 2014
SWV	Antibody	2-20 pg/mL	Serum	Li and Yang 2011
DPV	Antibody	0.5-100000 pg/mL	Serum	Peng et al. 2011
PEI	Antibody	1-100000 pg/mL	Serum	Fan et al. 2014
ECL	Antibody	0.1-1000 pg/mL	Serum	Sardesai, Barron, and Rusling 2011
EIS	Antibody	0.03-22.5 pg/mL	Serum	Aydin, Aydin, and Sezginturk 2020
	Antibody	0.01–50 pg/mL	Serum	Aydin, Aydin, and Sezginturk 2021
EIS	Antibody	0.01-100 fg/mL	Serum	Yang et al. 2013
EIS	Aptasensor	1-15000000 pg/mL	Serum	Tertiş, et al. 2017
EIS	Aptasensor	1-100000 pg/mL	Serum	Tertiş, et al. 2019b
Amperometry	Aptasensor	0.021-2100 pg/mL	Serum	Chen et al. 2020
EIS	Aptasensor	5-100000 pg/mL	Serum	Tertiş, et al. 2019a
This work	Molecular imprinting polymer	0.02–2000000 pg/ mL	Serum	

Definitions: ASV, anodic stripping voltammetry; SWV, square wave voltammetry; DPV, differential pulse voltammetry; PEI, photoelectrochemical immunoassay; ECL, electrochemiluminescence; and EIS, electrochemical impedance spectroscopy.

concentrations of the target prepared in 100-fold diluted serum. The analytical performance was evaluated by calibration curves obtained using EIS (Figure S2).

Calibration curves were recorded for the MPPy and NPPy sensors and plotted as the charge transfer resistance by EIS versus the logarithm of the IL6 concentration from 0.02 pg/mL to 20 ng/mL. The charge transfer resistance of MPPy increased linearly with the IL6 concentration above 0.02 pg/mL (Figure S2), with an average slope of 0.017 kXmL/log[IL6, ng/mL and correlation coefficients higher than 0.985.

Curiously, contrary to the calibration curve of MPPy in PBS buffer in Figure 4, the slope is positive, showing an increase of the signal after protein binding. A possible explanation is the presence of compounds in the serum that interact with the protein and change the net charge of the outer amino acids (Figure S2). Moreover, the biosensor recognized the protein because within the observed concentration range, the response of the MIPPy was dominated by the interaction of IL6 with the binding sites once a linear response was observed for the sensor versus the protein concentration. The NPPy material displayed a random response for the same protein concentration range, confirming that the primary mechanism of protein binding in the MPPy sensor is associated with the cavities present in the matrix.

Overall, considering that the cutoff levels of IL6 in serum are approximately 1.6 pg/ mL in healthy people (Wu et al. 2015) and higher in Alzheimer's patients, the analytical figures of merit have clinical significance. These results demonstrate that the developed biosensor can be effectively used for IL6 determination with good sensitivity. The analytical features of

the biosensor are compared to previously reported electrochemical biosensors in Table 1. The analytical performance of the MPPy sensor is equivalent to the literature devices for natural antibodies. However, the reported approach offers advantages in stability, cost, and response time.

Conclusions

The present work describes the development of an analytical device with integration of molecular imprinting of proteins and electrochemical transduction. The target is a biomarker associated with neuro-inflammation, the IL6 protein, which may be an indicator of the presence of Alzheimer's disease when associated with other symptoms.

The MIP biosensor was constructed by the electropolymerization of pyrrole performed by cyclic voltammetry on a C-SPE in the presence of the IL6. The template removal from the polymeric matrix was carried out by acid cleavage, giving rise to the imprinted sites.

The best conditions for the synthesis of the biomimetic material were obtained using a potential range from 0.8 to 0.8 V for 10 cycles and a scan rate of 50 mV/s. The monomer concentration is important in the imprinting process. The best conditions were obtained for 0.1 M Py. Selective binding of IL6 onto the MPPy sensor after 30 min incubation significantly modified the redox probe current. Calibration plots showed a linear dependence of peak current with linearity up to 0.02 pg/mL, an average slope of 0.017 kX mL/log[IL6, ng/mL] and correlation coefficients exceeding 0.985 in spiked serum samples.

Overall, this biomimetic material is more stable and robust compared to traditional immunosensors and ELISA methods, and simple, rapid, accuracte, and offers a low detection limit. This approach opens horizons for the rapid point-of-care diagnosis of biomarkers associated with Alzheimer's disease and with other conditions.

Acknowledgements

POCTEP/INTERREG is acknowledged through the project 2QBioneuro, Impulso de una red de I þ i en quımica biologica para diagn ostico y tratamiento de enfermedades neurol ogicas. ERA- Net, FCT/JPND cofunded Oligomer-Focused Screening and Individualized Therapeutics to target Neurodegenerative Disorders.

References

Algieri, C., E. Drioli, L. Guzzo, and L. Donato. 2014. Bio-Mimetic Sensors Based on Molecularly Imprinted Membranes. Sensors (Basel, Switzerland) 14 (8):13863–912. doi:10.3390/s140813863.

Aydin, E. B., M. Aydin, and M. K. Sezginturk. 2020. The development of an ultra-sensitive electrochemical immunosensor using a PPyr-NHS functionalized disposable ITO sheet for the detection of interleukin 6 in real human serums. New Journal of Chemistry 44:14228–38.

Aydin, E. B., M. Aydin, and M. K. Sezginturk. 2021. A novel electrochemical immunosensor based on acetylene black/epoxy-substituted-polypyrrole polymer composite for the highly sensitive and selective detection of interleukin 6. Talanta 222:121596.

Balducci, C., G. Santamaria, P. L. Vitola, E. Brandi, F. Grandi, A. R. Viscomi, M. Beeg, M. Gobbi, M. Salmona, S. Ottonello, et al. 2018. Doxycycline counteracts neuroinflammation restoring memory in Alzheimer's disease mouse models. Neurobiology of Aging 70:128–39. doi: 10.1016/j.neurobiolaging.2018.06.002.

Berkenbosch, F., J. Biewenga, M. Brouns, J. M. Rozemuller, P. Strijbos, and A. M. van Dam. 1992. Cytokines and inflammatory proteins in Alzheimer's Disease. Research in Immunology 143 (6):657–63. doi:10.1016/0923-2494(92)80052-M.

Cabinio, M., M. Saresella, F. Piancone, F. LaRosa, I. Marventano, F. R. Guerini, R. Nemni, F. Baglio, and M. Clerici. 2018. Association between Hippocampal Shape, Neuroinflammation, and Cognitive Decline in Alzheimer's Disease. Journal of Alzheimer's Disease 66 (3):1131–44. doi:10.3233/JAD-180250.

Cabral-Miranda, G., M. Gidlund, and M. G. F. Sales. 2014. Backside-surface imprinting as a new strategy to generate specific plastic antibody materials. Journal of Materials Chemistry. B 2 (20):3087–95. doi:10.1039/c3tb21740j.

Chen, W., Y. Ma, J. M. Pan, Z. H. Meng, G. Q. Pan, and B. Sellergren. 2015. Molecularly Imprinted Polymers with Stimuli-Responsive Affinity: Progress and Perspectives. Polymers. Polymers 7 (9):1689–715. doi:10.3390/polym7091478.

Chen, L., X. Wang, W. Lu, X. Wu, and J. Li. 2016. Molecular imprinting: Perspectives and applications. Chemical Society Reviews 45 (8):2137–211. doi:10.1039/c6cs00061d.

Chen, N., H. Yang, Q. Li, L. J. Song, S. C. B. Gopinath, and D. Wu. 2020. An interdigitated aptasensor to detect interleukin-6 for diagnosing rheumatoid arthritis in serum. Biotechnology and Applied Biochemistry :33244818.

Cross, A. H., A. Herman, D. Fiore, C. Harp, B. Musch, and A. Bar-Or. 2017. CSF cell signature and biomarkers of neuroinflammation and neurodegeneration in MS: Preliminary results of the OBOE study. Multiple Sclerosis Journal 23:837–8.

Daniels, J.S. and N. Pourmand, 2007. Label-free impedance biosensors: Opportunities and challenges. Electroanalysis 19, 1239–1257.

Day, G. S., F. Amtashar, M. L. Yarbrough, P. Kortvelyessy, H. Pruss, R. C. Bucelli, M. J. Fritzler, W. Mason, D. F. Tang-Wai, C. Steriade, et al. 2018. Quantifying Biomarkers of Neuronal Injury, Neuroinflammation and Neurotransmission in Antibody-Mediated Encephalitis. Annals of Neurology 84:S39–S40.

Fan, G. C., X. L. Ren, C. Zhu, J. R. Zhang, and J. J. Zhu. 2014. A new signal amplification strategy of photoelectrochemical immunoassay for highly sensitive interleukin-6 detection based on TiO2/CdS/CdSe dual co-sensitized structure. Biosensors & Bioelectronics 59:45–53. doi:10.1016/j.bios.2014.03.011.

Finneran, D. J., and K. R. Nash. 2019. Neuroinflammation and fractalkine signaling in Alzheimer's disease. Journal of Neuroinflammation 16 (1):8. doi:10.1186/s12974-019-1412-9.

Frasco, M. F., L. Truta, M. G. F. Sales, and F. T. C. Moreira. 2017. Imprinting Technology in Electrochemical Biomimetic Sensors. Sensors 17 (3):523–9. doi:10.3390/s17030523.

Gomes, R. S., F. T. C. Moreira, R. Fernandes, and M. G. F. Sales. 2018. Sensing CA 15-3 in point-of-care by electropolymerizing O-phenylenediamine (oPDA) on Au-screen printed electrodes. Plos One 13 (5):e0196656–19. doi:10.1371/journal.pone.0196656.

Haupt, K., A. V. Linares, M. Bompart, and T. S. B. Bernadette. 2012. Molecularly Imprinted Polymers. Topics in Current Chemistry 325:1–28. doi:10.1007/128_2011_307.

Huang, J. F., H. Chen, W. B. Niu, D. W. H. Fam, A. Palaniappan, M. Larisika, S. H. Faulkner, C. Nowak, M. A. Nimmo, B. Liedberg, et al. 2015. Highly manufacturable graphene oxide biosensor for sensitive interleukin-6 detection. RSC Advances 5 (49):39245–51. doi:10.1039/ C5RA05854F.

Huang, J. F., J. Harvey, W. H. D. Fam, M. A. Nimmo, and I. Y. A. Tok. 2013. Novel biosensor for Interleukin-6 detection. In: Chan, K. M., A. Subic, F. K. Fuss, and P. Clifton (Eds.), 6th Asia-Pacific Congress on Sports Technology: 195–200.

Janelidze, S., N. Mattsson, E. Stomrud, O. Lindberg, S. Palmqvist, H. Zetterberg, K. Blennow, and O. Hansson. 2018. CSF biomarkers of neuroinflammation and cerebrovascular dysfunction in early Alzheimer disease. Neurology 91 (9):E867–E877. doi:10.1212/WNL.0000000000006082.

Khosravi, F., S. M. Loeian, and B. Panchapakesan. 2017. Ultrasensitive Label-Free Sensing of IL-6 Based on PASE Functionalized Carbon Nanotube Micro-Arrays with RNA-Aptamers as Molecular Recognition Elements. Biosensors 7 (4):17–3. doi:10.3390/bios7020017.

Lakhin, A. V., V. Z. Tarantul, and L. V. Gening. 2013. Aptamers: Problems, Solutions and Prospects. Acta Naturae 5 (4):34–43.

Liu, P.-Z., X.-W. Hu, C.-J. Mao, H.-L. Niu, J.-M. Song, B.-K. Jin, and S.-Y. Zhang. 2013. Electrochemiluminescence immunosensor based on graphene oxide nanosheets/polyaniline nanowires/CdSe quantum dots nanocomposites for ultrasensitive determination of human interleukin-6. Electrochimica Acta 113:176–80. doi:10.1016/j.electacta.2013.09.074.

Li, T., and M. H. Yang. 2011. Electrochemical sensor utilizing ferrocene loaded porous polyelectrolyte nanoparticles as label for the detection of protein biomarker IL-6. Sensors and Actuators B: Chemical 158 (1):361–5. doi:10.1016/j.snb.2011.06.035.

Li, Q. R., K. G. Yang, Y. Liang, B. Jiang, J. X. Liu, L. H. Zhang, Z. Liang, and Y. K. Zhang. 2014. Surface Protein Imprinted Core-Shell Particles for High Selective Lysozyme Recognition Prepared by Reversible Addition-Fragmentation Chain Transfer Strategy. ACS Appl Mater Interfaces 6 (24):21954–60. doi:10.1021/am5072783.

Lou, Y., T. He, F. Jiang, J.-J. Shi, and J.-J. Zhu. 2014. A competitive electrochemical immunosensor for the detection of human interleukin-6 based on the electrically heated carbon electrode and silver nanoparticles functionalized labels. Talanta 122:135–9. doi:10.1016/j.talanta.2014.01.016.

Marttinen, M.,. M. Takalo, T. Natunen, R. Wittrahm, S. Gabbouj, S. Kemppainen, V. Leinonen, H. Tanila, A. Haapasalo, and M. Hiltunen. 2018. Molecular Mechanisms of Synaptotoxicity and Neuroinflammation in Alzheimer's Disease. Frontiers in Neuroscience 12:963 doi:10.3389/fnins.2018.00963.

Moreira, F. T. C., S. Sharma, R. A. F. Dutra, J. P. C. Noronha, A. E. G. Cass, and M. G. F. Sales. 2013. Smart plastic antibody material (SPAM) tailored on disposable screen printed electrodes for protein recognition: Application to myoglobin detection. Biosens Bioelectron 45:237–44. doi:10.1016/j.bios.2013.02.012.

Munge, B. S., C. E. Krause, R. Malhotra, V. Patel, J. S. Gutkind, and J. F. Rusling. 2009. Electrochemical immunosensors for interleukin-6. Comparison of carbon nanotube forest and gold nanoparticle platforms. Electrochemistry Communications 11 (5):1009–12. doi:10.1016/j.elecom.2009.02.044.

Ojeda, I., M. Moreno-Guzman, A. Gonzalez-Cortes, P. Yanez-Sedeno, and J. M. Pingarron. 2014. Electrochemical magnetoimmunosensor for the ultrasensitive determination of interleukin-6 in saliva and urine using poly-HRP streptavidin conjugates as labels for signal amplification. Analytical and Bioanalytical Chemistry 406 (25):6363–71. doi:10.1007/s00216-014-8055-6.

Park, J. C., S. H. Han, and I. Mook-Jung. 2020. Peripheral inflammatory biomarkers in Alzheimer's disease: A brief review. BMB Reports 53 (1):10–9. doi:10.5483/BMBRep.2020.53.1.309.

Peng, J., L.-N. Feng, Z.-J. Ren, L.-P. Jiang, and J.-J. Zhu. 2011. Synthesis of Silver NanoparticleHollow Titanium Phosphate Sphere Hybrid as a Label for Ultrasensitive Electrochemical Detection of Human Interleukin-6. Small (Weinheim an Der Bergstrasse, Germany) 7 (20): 2921–8. doi:10.1002/smll.201101210.

Popp, J., A. Oikonomidi, D. Tautvydaite, L. Dayon, M. Bacher, E. Migliavacca, H. Henry, R._ Kirkland, I. Severin, J. Wojcik, et al. 2017. Markers of neuroinflammation associated with Alzheimer's disease pathology in older adults. Brain, Behavior, and Immunity 62:203–11. doi:10.1016/j.bbi.2017.01.020.

Ribeiro, J. A., C. M. Pereira, A. F. Silva, and M. G. F. Sales. 2018. Disposable electrochemical detection of breast cancer tumour marker CA 15-3 using poly(Toluidine Blue) as imprinted polymer receptor. Biosensors & Bioelectronics 109:246–54. doi:10.1016/j.bios.2018.03.011.

Sardesai, N. P., J. C. Barron, and J. F. Rusling. 2011. Carbon Nanotube Microwell Array for Sensitive Electrochemiluminescent Detection of Cancer Biomarker Proteins. Analytical Chemistry 83 (17):6698–703. doi:10.1021/ac201292q.

Sayyah, S. M., S. S. Abd El-Rehim, and M. M. El-Deeb. 2003. Electropolymerization of pyrrole and characterization of the obtained polymer films. Journal of Applied Polymer Science 90 (7): 1783–92. doi:10.1002/app.12793.

Shi, J. J., T. T. He, F. Jiang, E. S. Abdel-Halim, and J. J. Zhu. 2014. Ultrasensitive multi-analyte electrochemical immunoassay based on GNR-modified heated screen-printed carbon electrodes and PS@PDA-metal labels for rapid detection of MMP-9 and IL-6. Biosensors & Bioelectronics 55:51–6. doi:10.1016/j.bios.2013.11.056.

Suk, K. 2006. Proteomics-based discovery of biomarkers and therapeutic targets in neurodegenerative diseases: Perspective of microglia and neuroinflammation. Expert Opinion on Therapeutic Patents 16 (3):237–47. doi:10.1517/13543776.16.3.237.

Tavares, A. P. M., and M. G. F. Sales. 2018. Novel electro-polymerized protein-imprinted materials using Eriochrome black T: Application to BSA sensing. Electrochimica Acta 262:214–25. doi:10.1016/j.electacta.2017.12.191.

Terti¸s, M., B. Ciui, M. Suciu, R. Sandulescu, and C. Cristea. 2017. Label-free electrochemical aptasensor based on gold and polypyrrole nanoparticles for interleukin 6 detection. Electrochimica Acta 258:1208–18. doi:10.1016/j.electacta.2017.11.176.

Terti¸s, M., P. I. Leva, D. Bogdan, M. Suciu, F. Graur, and C. Cristea. 2019. Impedimetric aptasensor for the label-free and selective detection of interleukin-6 for colorectal cancer screening. Biosensors & Bioelectronics 137:123–32. doi:10.1016/j.bios.2019.05.012.

Terti¸s, M., G. Melinte, B. Ciui, I. S¸imon, R. S¸tiufiuc, R. Sandulescu, and C. Cristea. 2019b. A Novel Label Free Electrochemical Magnetoimmunosensor for Human Interleukin-6 Quantification in Serum. Electroanalysis 31 (2):282–92. doi:10.1002/elan.201800620.

Tsuneyasu, M., C. Sasakawa, N. Naruishi, Y. Tanaka, Y. Yoshida, and K. Tawa. 2014. Sensitive detection of interleukin-6 on a plasmonic chip by grating-coupled surface-plasmon-fieldenhanced fluorescence imaging. Japanese Journal of Applied Physics 53 (6S):06JL05. 16p_D5_9. doi:10.7567/JJAP.53.06JL05.

Uzun, L., and A. P. F. Turner. 2016. Molecularly-imprinted polymer sensors: Realising their potential. Biosensors & Bioelectronics 76:131–44. doi:10.1016/j.bios.2015.07.013.

Wang, G., H. Huang, G. Zhang, X. Zhang, B. Fang, and L. Wang. 2011. Dual Amplification Strategy for the Fabrication of Highly Sensitive Interleukin-6 Amperometric Immunosensor Based on Poly-Dopamine. Langmuir : The ACS Journal of Surfaces and Colloids 27 (3): 1224–31. doi:10.1021/la1033433.

Wang, C. W., U. Manne, V. B. Reddy, D. K. Oelschlager, V. R. Katkoori, W. E. Grizzle, and R. Kapoor. 2010. Development of combination tapered fiber-optic biosensor dip probe for quantitative estimation of interleukin-6 in serum samples. Journal of Biomedical Optics 15 (6):067005 doi:10.1117/1.3523368.

Wu, Y. Y., J. L. Hsu, H. C. Wang, S. J. Wu, C. J. Hong, and I. H. J. Cheng. 2015. Alterations of the Neuroinflammatory Markers IL-6 and TRAIL in Alzheimer's Disease. Dementia and Geriatric Cognitive Disorders Extra 5 (3):424–34. doi:10.1159/000439214.

Yang, T., S. Wang, H. Jin, W. Bao, S. Huang, and J. Wang. 2013. An electrochemical impedance sensor for the label-free ultrasensitive detection of interleukin-6 antigen. Sensors and Actuators B: Chemical 178:310–5. doi:10.1016/j.snb.2012.12.107.

Zhang, J. J., Y. Liu, L. H. Hu, L. P. Jiang, and J. J. Zhu. 2011. "Proof-of-principle" concept for ultrasensitive detection of cytokines based on the electrically heated carbon paste electrode . Chemical Communications (Cambridge, England) 47 (23):6551–3. doi:10.1039/c1cc11565k.